Medical Physics
The International Journal of Medical Physics Research and Practice

Computerized threedimensional segmented human anatomy

I. George Zubal, Charles R. Harrell, Eileen O. Smith, Zachary Rattner, Gene Gindi, and Paul B. Hoffer

Citation: Medical Physics **21**, 299 (1994); doi: 10.1118/1.597290
View online: http://dx.doi.org/10.1118/1.597290
View Table of Contents: http://scitation.aip.org/content/aapm/journal/medphys/21/2?ver=pdfcov
Published by the American Association of Physicists in Medicine

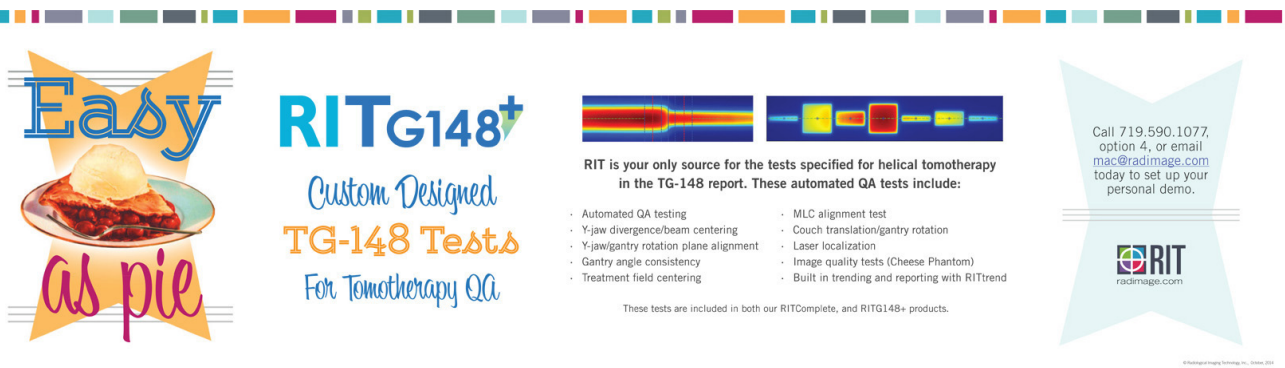

Computerized three-dimensional segmented human anatomy

I. George Zubal,[a] Charles R. Harrell, Eileen O. Smith, Zachary Rattner, Gene Gindi, and Paul B. Hoffer
Imaging Science Research Laboratories, Department of Diagnostic Radiology, Yale University School of Medicine, New Haven, Connecticut 06510

(Received 25 November 1992; accepted for publication 27 October 1993)

Manual segmentation of 129 x-ray CT transverse slices of a living male human has been done and a computerized 3-dimensional volume array modeling all major internal structures of the body has been created. Each voxel of the volume contains a index number designating it as belonging to a given organ or internal structure. The original x-ray CT images were reconstructed in a 512×512 matrix with a resolution of 1 mm in the x,y plane. The z-axis resolution is 1 cm from neck to midthigh and 0.5 cm from neck to crown of the head. This volume array represents a high resolution model of the human anatomy and can serve as a voxel-based anthropomorphic phantom suitable for many computer-based modeling and simulation calculations.

Key words: segmentation, human model, anthropomorphic phantom, x-ray CT

I. INTRODUCTION

Models of the human anatomy serve an important role in several aspects of diagnostic and therapy related image processing. Computerized anthropomorphic phantoms can either be defined by mathematical (analytical) functions, or digital (voxel-based) volume arrays.

One of the earliest computerized anthropomorphic phantoms was developed for estimating doses to various human organs from internal or external sources of radioactivity and served to calculate the S factors for internal dose calculations in nuclear medicine.[1] This mathematical phantom models internal structures as either ellipsoids, cylinders, or rectangular volumes. For internal dosimetry purposes, such human model approximations serve quite sufficiently and have the advantage of allowing very fast calculation of the intersection of ray lines with the analytical surfaces which delineate the organs. A version of this mathematical phantom has been updated to include female organs.[2] There are additionally versions (personal communication, Benjamin M. Tsui, Ph.D., Dept. of Radiology, Univ. of North Carolina) of the phantom which are used for dedicated cardiac studies where the structures adjacent to the heart and the heart itself have been more realistically modeled.[3]

Computer models have also been applied to better understand the image formation process in diagnostic radiology,[4–7] particularly for analyzing scatter and attenuation problems in nuclear medicine.[8–14] Since much higher statistics are necessary to model imaging simulations (compared to dosimetry simulations), speed of computing individual gamma ray histories becomes of paramount importance for imaging physics calculations. The software phantoms modeled in these imaging simulations have sometimes been limited to simple point, rod, and slab shapes of sources and attenuating media. Such simple geometries are useful in studying more fundamental issues of scatter and attenuation; but, clinically realistic distributions cannot be adequately evaluated by such simple geometries. The intricate protuberances and convolutions of human internal structures are important in evaluating imaging techniques; and as the resolution of imaging equipment improves, it is essential to enhance our computer models.

In the field of oncology, internal and external radiotherapy sources have become more sophisticated in their design and applications. The calculations involved in clinical therapy planning have become more sophisticated.[15–18] These new therapy techniques can be more effectively investigated with higher resolution, computerized realistic human models.

In order to make 3-dimensional anatomical data suitable for use in any of these radiologic calculations, we must be able to delineate the surfaces and internal volumes which define the various structures of the body. These segmented volumes can then be indexed to activity distributions or other physical characteristics (density or elemental composition). We have constructed an anatomically correct human geometry for use in these types of radiologic calculations where each organ (structure) is segmented and its internal volume is referenced by an index number.

II. METHODS

A. Anatomic data

Transmission computerized x-ray tomography (CT) supplies us the required high resolution 3-dimensional human anatomy necessary to construct the volume segmented phantom. A considerable number of patients are imaged from head to midthigh in our hospital to study diffuse diseases. We selected an adult male whose dimensions were similar to the dosimetry standard mathematical phantom.[1] Our selected patient's height was 5 foot 10 inches and weight was 155 pounds. He was scheduled for head, thorax, abdomen, and pelvic scans for diagnosis of diffuse melanoma. The patient had no advanced signs of disease or obvious lesions nor advanced symptoms during

 0094-2405/94/21(2)/299/4/$1.20

TABLE I. List of organ index numbers and respective organs or structures segmented in the human phantom.

Organ numbers for the torso	
0—Void outside of phantom	18—Small intestine
1—Skin/body fat	19—Colon/Large intestines
2—Brain	20—Pancreas
3—Spinal chord	21—Adrenals
4—Skull	22—Fat
5—Spine	23—Blood pool (all vessels)
6—Rib cage and sternum	24—Gas volume (bowel)
7—Pelvis	25—Fluid volume (bowel)
8—Long bones	26—Bone marrow
9—Skeletal muscle	27—Lymph nodes
10—Lungs	28—Thyroid
11—Heart	29—Trachea
12—Liver	30—Diaphram
13—Gallbladder	31—Spleen
14—Left and right kidney	32—Urine
15—Bladder	33—Feces (colon contents)
16—Esophagus	34—Testes
17—Stomach	35—Prostate
	36—Liver lesion

the time of the scans. After informing the patient of the potential application of his scans for biomedical research purposes, he agreed to release his scan data for research purposes. The standard clinical imaging protocol was carried out. Using the GE 9800 Quick Scanner, a total of 78 slice images were acquired from neck to midthigh with a 1-cm slice thickness using a 48-cm field of view (pixel size=1 mm). During a second imaging session, 51 slices of the same patient were acquired of the head and neck region with 5-mm slice thickness and a field of view of 24 cm (pixel size=0.5 mm). The body and head slices were transferred to our image processing lab by reading the reconstructed transverse slices from the CT archive reel to reel magnetic tape, decompressing the images from the manufacturer's lossless storage format, and storing them in expanded matrix format on disk.

B. Organ delineation

The data access and processing programs were created on a VAX 3500 workstation running VMS version 5.0-2 using the available User Interface Services (UIS routines) for program control of the resident color display screen. The color display monitor is a 1024 by 1024 pixel raster display equipped with 8 bit planes. One bit plane is used for overlay graphics while the remaining 7 bits are used for mapping 128 color levels to the displayed transverse images. A serial line high resolution Summagraphics bitpad provided high resolution cursor control. An in-house program was developed to read the transverse slices from disk, display them on the color workstation monitor, and permit outlining of organs under bitpad cursor control. The x and y integer positions of all of the organ outlines are stored on disk with a resolution of 512 by 512 pixels. Members of the medical staff outlined 35 separate internal organs (see Table I) and known structures contained in the transverse slices. A region of interest coloring routine was used to fill the inside of each organ outline with a unique index value. Default lesions of approximately 0.5, 1.0, and 2.0 cm diam were arbitrarily defined at three locations in the liver. A total of more than one thousand contours were drawn with 1-mm resolution to define this fully 3-dimensional voxel phantom of the human. Since the original CT images are still available, the original Hounsfield numbers are also known for each voxel in the defined structures. The scanner used is a clinical instrument; the accuracy of the Hounsfield numbers is assured through the routine maintenance and calibration carried out for quality assurance.

The segmented image information is stored in two independent files. A variable size file is created for each transverse slice and contains the x,y coordinates of each of the contours drawn on that slice. The slice number is retained in the name of the file.These contours serve as the input to the filling routine, which creates a fixed size organ index image. The organ index image is a 512 by 512 byte matrix filled with integer values which delineate the internal structures (organs) of the body. the organ index image is therefore, in effect, the original CT transverse slice in which the Hounsfield numbers are replaced by integers corresponding to the organ index value. The assignment of integers to the organs are shown in Table I.

C. Data access and display

The 2-dimensional organ index slice images can be read into a 512 by 512 by 119 voxel 3-dimensional array, in which the x,y resolution is 1 mm per pixel and the slice thickness is 10 mm in the body and 5 mm in the head. The reduction from 129 to 119 slices is due to the overlap of information in the neck region. In order to make the data more manageable and to have consistent voxel dimensions along all three axes, we routinely transform the original data into a $128\times128\times246$ matrix where the isotropic cubic voxel resolution is 4 mm on each side. This volume array is created by combining pixels in the x,y plane and by duplicating slices along the z direction. In order to remove some of the blocky appearance created in the torso by duplicating voxels along the z direction, we applied 3-dimensional modal filtering. In our application of modal filtering a subvolume of 5 by 5 by 5 voxels was selected out of the original phantom volume. The central voxel's filtered value was calculated as the mode (most often occurring) value from the selected 125 subvolume.

The total storage capacity of the files are: original CT images=29 Megabyte, x,y contours=1 Megabyte, organ index matrices 20 Megabytes, and are available for public access through our Imaging Science Research Laboratory. (In order to gain access to the phantom data, please send your request to Dr. George Zubal. E-mail: Zubal@BioMed.Med.Yale.Edu.)

III. RESULTS

In order to appreciate the detail of the anthropomorphic phantom, we projected anterior and lateral views of selected structures from the $128\times128\times246$ volume. This was done by replacing selected index numbers with a pos-

FIG. 1. Anterior and lateral projections of the 3-dimensional segmented human phantom. The skin and fat (index number = 1) are highlighted to show the outline of the patient as well as internal bones (corresponding to index numbers: 4, 5, 6, 7, and 8).

FIG. 2. Anterior and lateral projections highlighting the skin and fat (index number = 1) as well as the brain (2), lungs (10), bladder and ureters (15).

itive integer value and setting other (unselected) structures to 0. The 3-dimensional volume was then collapsed parallel to the major axes onto two 2-dimensional matrices (each collapsed matrix = 128×246) by adding all integer values along rows of voxels. The final matrices were normalized and displayed using a gray scale color table and are shown in Figs. 1–3. All figures are rendered with the skin/fat voxels selected in order to show the outline of the patient's body; within this outline, various structures are selected for display.

IV. DISCUSSION

We have created a digital voxel-based phantom which closely resembles a typical male anatomy. Organ outlines were manually drawn with millimeter resolution in each of 129 transverse slice images of the human torso. Such an anthropomorphic 3-dimensional phantom has several interesting applications in the radiological sciences. We have routinely used the voxel-based phantom in Monte Carlo simulations to yield diagnostically realistic images of internal distributions of radiopharmaceuticals.[19,20] Since we are able to model a known source distribution and known attenuator distribution, the Monte Carlo simulations give us projection data which not only closely resemble clinical data, but include additional information not determinable in patient studies. Such data sets can help to better understand the image formation process for clinically realistic models, and can prove especially interesting in testing and improving tomographic reconstruction algorithms.[21]

New imaging devices can be investigated using "in vivo" simulations. The tumor detection capabilities of a novel coincidence counting probe system has been investigating using the anthropomorphic phantom described here.[22] Early design changes can be realized before studies are conducted in living models. One of the advantages of developing this very realistic human model is that such sim-

FIG. 3. Anterior and lateral projections highlighting the skin and fat (index number = 1), and myocardium of the heart (11).

ulations can decrease the necessity of conducting experimental studies using animal models—particularly primates.

Dose calculations for internal and external radiation sources using this phantom can give new insights in the field of health physics and therapy. We hope to extend the application of this phantom to therapy related simulations.

ACKNOWLEDGMENTS

Work performed under Contract No. DE FG02-88ER60724 with the U. S. Department of Energy. We are thankful to Mindy Lee, whose computer programming skills were essential for outlining and storing the segmented data. We are indebted to Cornelius N. de Graaf, Utrecht, The Netherlands, for his implementation of the volumetric smoothing.

[a]Corresponding author: I. George Zubal, Yale University School of Medicine, Department of Diagnostic Radiology, BML 332, 333 Cedar Street, New Haven, CT 06510.

[1]W. Snyder, M. R. Ford, and G. Warner, *Estimates of Specific Absorbed Fractions for Photon Sources Uniformly Distributed in Various Organs of a Heterogeneous Phantom*, NM/MIRD Pamphlet No. 5 (Society of Nuclear Medicine Publication, New York, 1978).

[2]G. Williams, M. Zankll, W. Abmayr, R. Veit, and G. Drexler, "The Calculation of Dose from External Photon Exposures using Reference and Realistic Human Phantoms and Monte Carlo Methods," Phys. Med. Bio. **31**, 449–452 (1986).

[3]H. Wang, R. J. Jaszczak, and R. E. Coleman, "Solid Geometry-Based Object Model for Monte Carlo Simulated Emission and Transmission Tomographic Imaging Systems," IEEE Trans. Med. Imaging **11**, 361–372 (1992).

[4]G. Barnea and C. E. Dick, "Monte Carlo studies of x-ray scatterings in transmission diagnostic radiology," Med. Phys. **16**, 490–495 (1986).

[5]H. P. Chan and K. Doi, "Physical characteristics of scattered radiation in diagnostic radiology: Monte Carlo simulation studies," Med. Phys. **12**, 152–165 (1985).

[6]H. Kanamori, N. Nakamori, and K. Inone, "Effects of scattered x-rays on CT images," Phys. Med. Bio. **30**, 239–249 (1985).

[7]D. R. Dance and G. J. Day, "The computation of scatter in mammography by Monte Carlo methods," Phys. Med. Bio. **29**, 237–247 (1984).

[8]J. Logan and H. J. Bernstein, "A Monte Carlo simulation of Compton scattering in positron emission tomography," J. Comput. Assist. Tomogr. **7**, 316–320 (1983).

[9]C. E. Floyd, R. S. Jaszczak, C. C. Harris, and R. E. Coleman, "Energy and spatial distribution of multiple order Compton scatter in SPECT. A Monte Carlo investigation," Phys. Med. Bio. **29**, 1217–1230 (1984).

[10]C. E. Floyd, R. J. Jaszczak, K. L. Greer, and R. E. Coleman, "Deconvolution of Compton scatter in SPECT," J. Nucl. Med. **26**, 403–408 (1985).

[11]C. E. Floyd, R. J. Jaszczak, K. L. Greer, and R. E. Coleman, "Inverse Monte Carlo as a Unified Reconstruction Algorithm for ECT," J. Nucl. Med. **27**, 1577–1585 (1986).

[12]C. E. Floyd, R. J. Jaszczak, K. L. Greer, and R. E. Coleman, "Brain Phantom: high resolution imaging with SPECT and I-123," Radiology **164**, 279–281 (1987).

[13]J. W. Beck, R. J. Jaszczak, R. E. Coleman, C. F. Starmer, and L. W. Nolte, "Analysis of SPECT Including Scatter and Attenuation Using Sophisticated Monte Carlo Modeling Methods," IEEE Trans. Nucl. Sci. **29**, 506–511 (1982).

[14]D. Acchiappati, N. Cerullo, and R. Guzzardi, "Assessment of the Scatter Fraction Evaluation Methodology using Monte-Carlo Simulation Techniques," European J. Nucl. Med. **15**, 683–686 (1989).

[15]M. Saxner, A. Trepp, and A. Ahnesjo, "A pencil beam model for photon dose calculation," Med. Phys. **19**, 263–273 (1992).

[16]A. S. Meigooni and R. Nath, "Tissue inhomogeneity correction for brachytherapy sources in a heterogeneous phantom with cylindrical symmetry," Med. Phys. **19**, 401–407 (1992).

[17]R. Mohan, G. Mageras, B. Baldwin, L. Brewster, G. Kutcher, S. Leibel, C. Burman, C. Long, and Z. Fuks, "Clinically relevant optimization of 3-D conformal treatments," Med. Phys. **19**, 933–944 (1992).

[18]D. Nigg, P. Randolph, and F. Wheeler, "Demonstration of three-dimensional deterministic radiation transport theory dose distribution analysis for boron neutron capture therapy," Med. Phys. **18**, 43–53 (1991).

[19]I. G. Zubal and C. H. Harell, "Voxel based Monte Carlo Calculations of Nuclear Medicine Images and Applied Variance Reduction Techniques," Image and Vision Computing **10**, 342–348 (1992).

[20]I. G. Zubal, C. R. Harrell, and P. D. Esser, "Monte Carlo determination of emerging energy spectra for diagnostically realistic radiopharmaceutical distributions," Nucl. Instrum. Methods Phys. Research **A299**, 544–547 (1990).

[21]G. S. Hademenos, M. A. King, M. Ljungberg, I. G. Zubal, and C. R. Harrell, "A Scatter Correction Method for T1201 Images: A Monte Carlo Investigation," *1992 IEEE Nuclear & Science Symposium and Medical Imaging Conference*, Oct. 25–31, 1992, Orlando, FL, Vol. 2, pp. 1213–1216.

[22]J. R. Saffer, H. H. Barrett, H. B. Barber, and J. M. Woolfenden, "Surgical Probe Design for a Coincidence Imaging System Without a Collimator," in *Proceedingss of the 12th International Conference on Information Processing in Medical Imaging* (Springer-Verlag, Berlin, 1991), pp. 8–22.